

Electronic Supplementary Material

Nitrogen and Fluorine Dual-Doped Porous Graphene-Nanosheets as Efficient Metal-Free Electrocatalysts for Hydrogen-Evolution in Acidic Media

Xin Yue^{a, b, ‡}, Shangli Huang^{a, ‡}, Yanshuo Jin^b, and Pei Kang Shen^{a, b *}

^aCollaborative Innovation Center of Sustainable Energy Materials, Guangxi University, Nanning 530004, P. R. China.

^bSchool of Materials Science and Engineering, Sun Yat-sen University, Guangzhou, 510275, P. R. China.

Email: stsspk@mail.sysu.edu.cn

[‡]These authors contributed equally.

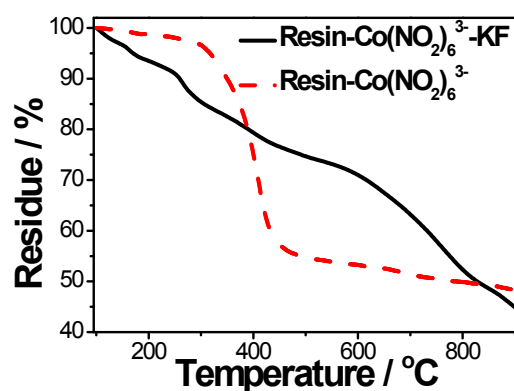


Fig. S1 TG curves of Resin-Co(NO₂)₆³⁺-KF and Resin-Na₃Co(NO₂)₆³⁺ samples under pure N₂ atmosphere with heating rate of 5 °C/min.

Inductively Coupled Plasma-atomic Emission Spectrometry (ICP) was performed to measure contents of Co in NFPGNS and NG. The results mean that residues of Co in catalysts are too little to act as active composition.

Table S1 Residue Co in NFPGNS and NG detected by ICP.

	Co mg/ 100 g
NFPGN	0.019
NG	0.184

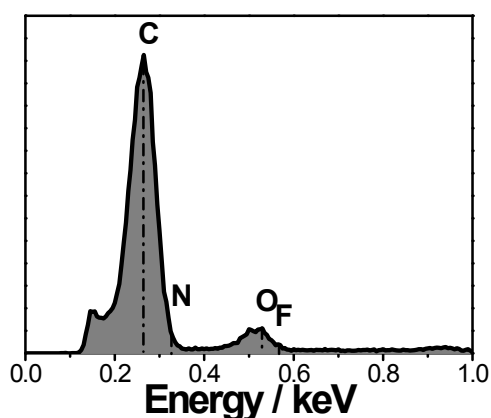


Fig. S2 The EDS pattern of NFPGNS.

Table S2 Ratios of three doped N configurations in NFPGNS and NG.

	NFPGNS / %	NG / %
Pyridinic N	64.9	24.82
Pyrrolic N	24.7	17.14
Graphitic N	10.4	58.04

The sintered temperature was found related to N and F doping level (Fig. S3). N and F doping level of samples sintered at different temperature was measured by XPS, indicating that N has been doped in grapheme structure below 700 °C based on the use of N containing anion exchanged resin and $\text{Na}_3\text{Co}(\text{NO}_2)_6$. Doping N escaped gradually with sintered temperature increased. However, F element doped in grapheme structure above 800 °C based on the melting point of KF is 858 °C. This means that F cannot be doped in the grapheme structure when solid state KF has not been melted. In contrast with doping of N, the amount of doping F increasing with sintered temperature increased.

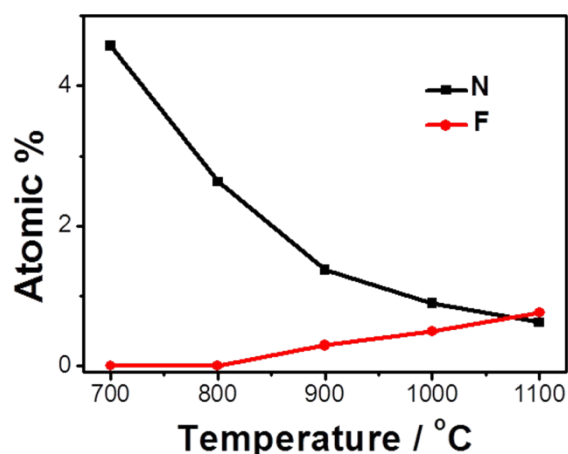


Fig. S3 Doping levels of N and F elements at different temperature.

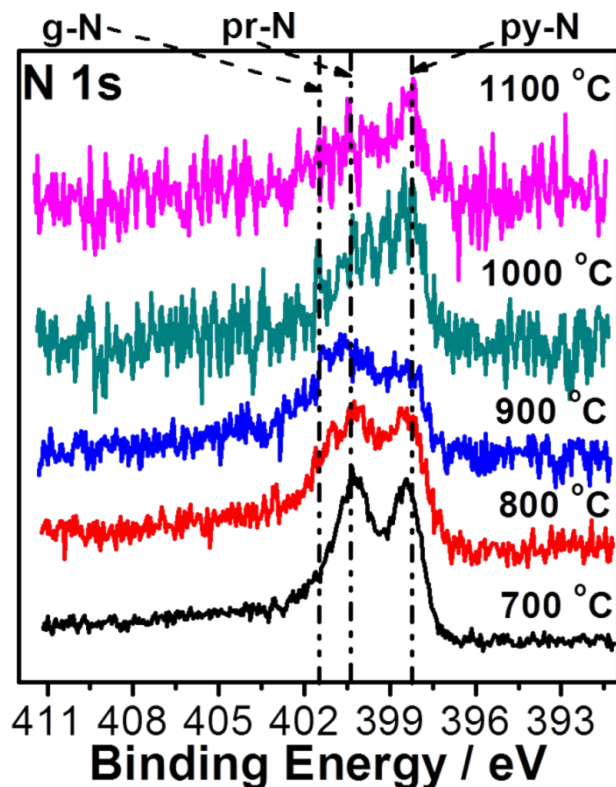


Fig. S4 XPS spectra of samples sintered at different temperature.

In the case of NG, the peak position at 284.6 eV is corresponding to C1 (sp^2 carbon), at 285.3 eV is corresponding to C2 (sp^3 carbon) and at 286.4 eV is attributed to C3 (C-O bond) in the case of C 1s spectrum (Fig. S5a). The N 1s spectrum can be analyzed to three configurations: pyridinic N at 398.1 eV, pyrrolic N at 400.5 eV and graphitic N at 401.3 eV (Fig. S5b). NG exhibits a graphitic N dominated doping structure (Table S2). No evidence proved existence of F element in NG (Fig. S5c). In the case of O 1s spectrum, the peak at 534 eV corresponds to oxygen in carboxyl groups, the peak at 532 eV attributed to carbonyl oxygen atoms in esters, amides, carboxylic anhydrides and oxygen atoms in hydroxyls or ethers, and at 531 eV associated with C=O groups such as ketone, lactone, and carbonyl groups (Fig. S5d).

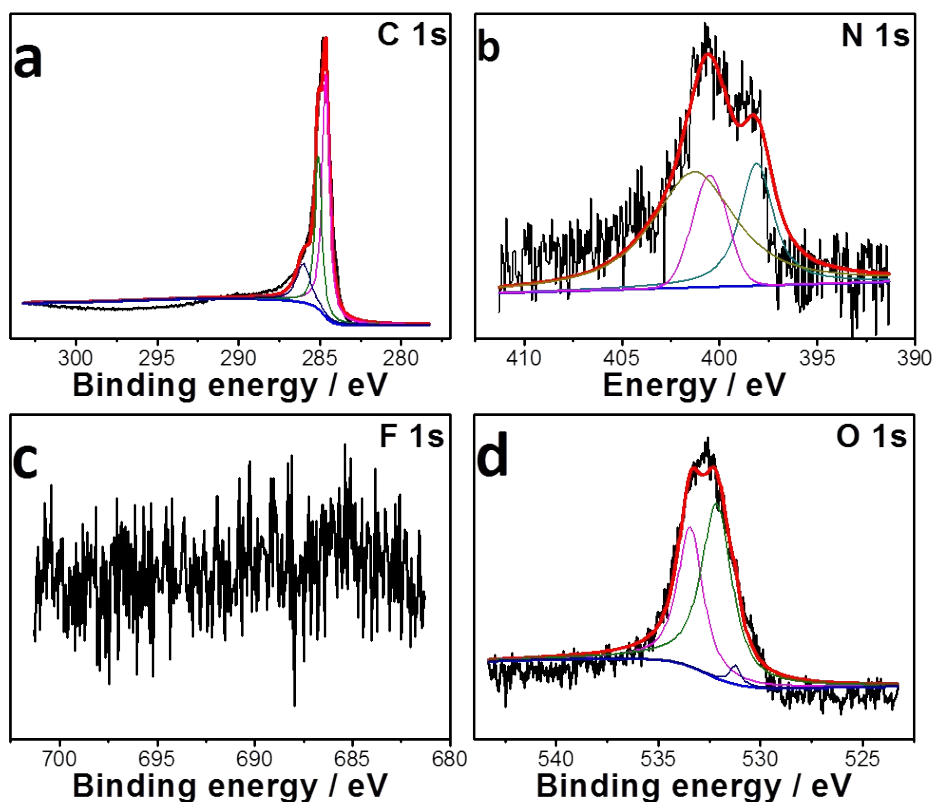


Fig. S5 XPS spectra of NG.

In the case of FC, the peak position at 284.6 eV is corresponding to C1 (sp^2 carbon), at 285.3 eV is corresponding to C2 (sp^3 carbon) and at 286.4 eV is attributed to C3 (C-O bond) in the case of C 1s spectrum (Fig. S6a). No evidence proved existence of N element (Fig. S6b). The peak in F 1s spectrum at 687.3 eV is attributed to C-F bond (Fig. S6c). In the case of O 1s spectrum, the peak at 534 eV corresponds to oxygen in carboxyl groups, the peak at 532 eV attributed to carbonyl oxygen atoms in esters, amides, carboxylic anhydrides and oxygen atoms in hydroxyls or ethers, and at 531 eV associated with C=O groups such as ketone, lactone, and carbonyl groups (Fig. S6d).

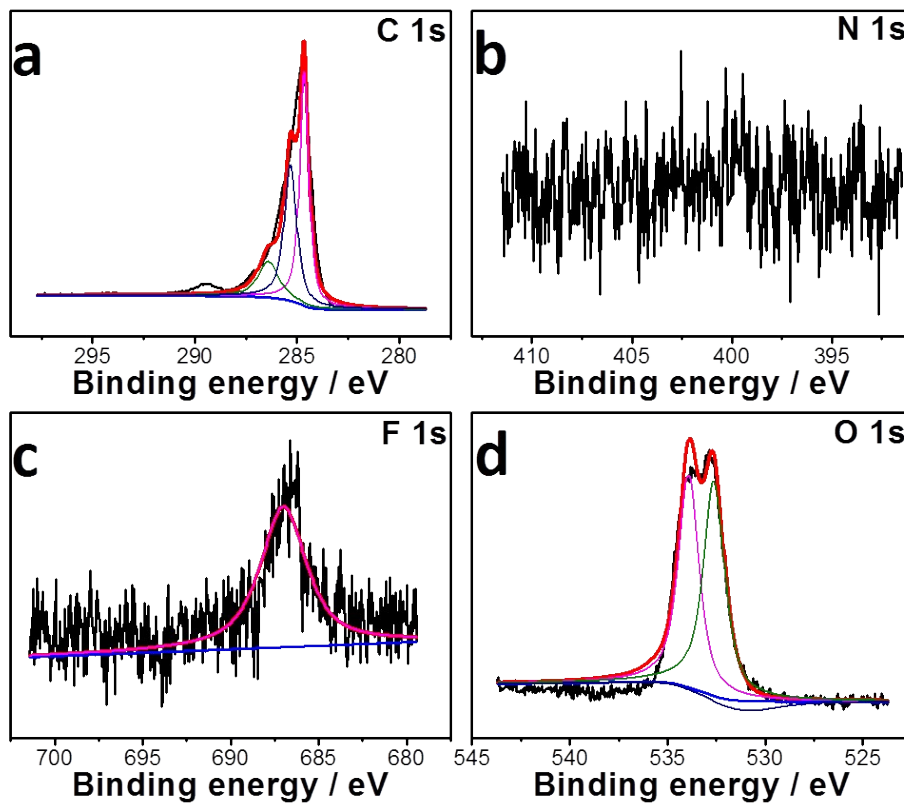


Fig. S6 XPS spectra of FC.

Fig. S7 shows CV curves of NFPGNS in 1 M HClO₄ at 25 °C with different scan rates from 1 to 200 mV s⁻¹. NFPGNS showed a very high specific capacity, especially at scan rate of 1 mV s⁻¹ (564 mF cm⁻²), based on its high surface area (BET surface area of 1340 m² g⁻¹). Meanwhile, there are no remarkable peaks in these CV curves.

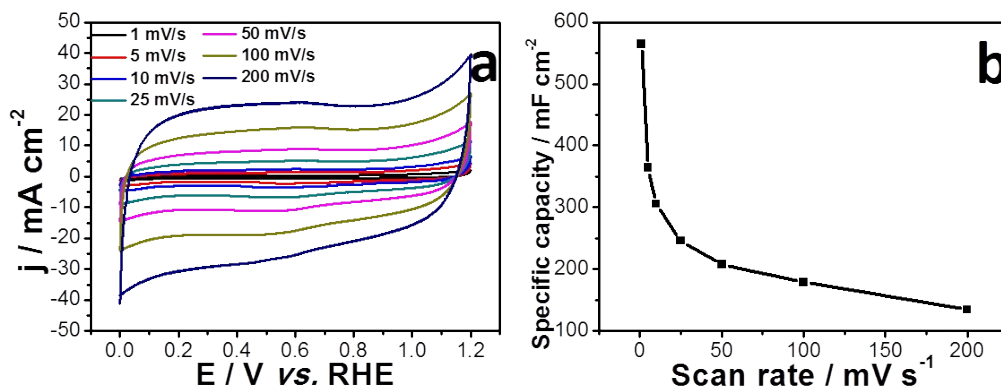


Fig. S7 (a) CV curves of NFPGNS in 1 M HClO₄ at 25 °C with different scan rate. (b)

Relationship between specific capacities and scan rates.

Electrochemical performances towards HER on NFPGNS, NG, FC, CC and Pt/C in this work were measured using a three-electrode-cell (Fig. S8a), with a *L*-shaped glassy carbon electrode ($\phi = 5$ mm) as the working electrode, a graphite rod as the counter electrode and a reversible hydrogen electrode (RHE) electrode as the reference electrode. The multi-step chronoamperometric curve for HER on NFPGNS electrocatalysts started at 50 mV *vs.* RHE and ended at -400 mV *vs.* RHE, with a decrement of 10 mV per step for 3 min without *iR*-correction (Fig. S8b).

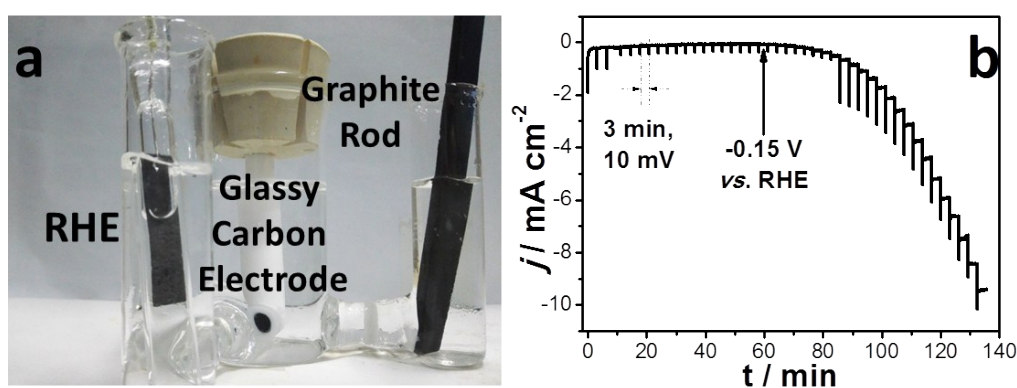


Fig. S8 (a) The three-electrode-system was used for measuring electrochemical performance of HER in this work. (b) Multi-step chronoamperometric curves for HER of NFPGNS in 1 M HClO₄ at 25 °C.

Exchange current density (j_0), as the most inherent measure of activity for HER, was always determined by fitting *i*-E data to the Tafel equation^{S1}. In this work, j_0 was also obtained by fitting *i*-E data to the Tafel equation and j_0 was the current density at overpotential of 0.

Table S3 HER performance on metal free electrocatalysts.

Catalyst	Electrolyte	Onset potential / V	Tafel slope / mV/dec	j_0 / mA/cm ²	η @ 10 mA cm ⁻² / V	Reference
N, P doped Graphene	0.5 M H ₂ SO ₄	-0.29	91	2.4×10^{-4}	-0.42	ACS Nano, 2014, 8, 5290 .
N, S co-doped Graphene	0.5 M H ₂ SO ₄	-0.22	105	N/A	-0.385	Angew. Chem. Int. Ed., 2015, 54, 2131.
B-SuG	0.5 M H ₂ SO ₄	~ -0.20	99	1.4×10^{-3}	N/A	Catal. Sci. Technol., 2014, 4, 2023.
C ₃ N ₄ @NG	0.5 M H ₂ SO ₄	N/A	51.5	3.5×10^{-4}	~ -0.240	Nat. Commun.; 2014, 5, doi:10.1038/ncomms4783.
C ₆₀ (OH) ₈	0.5 M H ₂ SO ₄	-0.16	103	N/A	N/A	Angew. Chem. Int. Ed. 2013, 52, 10867.
NFPGNS	1 M HClO ₄	-0.15	87	5.3×10^{-3}	-0.29	This work
NG	1 M HClO ₄	-0.20	106	9.7×10^{-4}	-0.37	This work
FC	1 M HClO ₄	-0.25	143	5.4×10^{-4}	N/A	This work
CC	1 M HClO ₄	N/A	159	1.0×10^{-4}	N/A	This work
Pt/C	1 M HClO ₄	~0	30	2.7×10^{-1}	-0.03	This work

NFPGNS sintered at 1000 °C exhibits best catalytic activity, showing a current density of -47.8 mA cm⁻² at -0.40 V vs. RHE (Fig. S9). Samples sintered below 900 °C exhibit worse catalytic activities; although pyridinic N and pyrrolic N dominated doping configurations and higher N doping level was observed (Fig. S4). This is

because that F has not doped in graphene or doping level is too little. The purpose of F doping in this work is increasing catalytic activities of N doped graphene by introducing modified electron acceptor-donor properties of carbons by synergistically coupling effect between heteroatoms with large number of C sites serving as active sites to adsorb adsorbates. However, it has been reported that fluorine modifies electronic properties of graphene by reducing the charge in conducting π orbitals with band gap level increased ^{S2}. This is detrimental to conductivity and even catalytic performance of F doped graphene. In fact, F doped sample and NFGNS sintered at 1100 °C with F as dominated heteroatoms showed worst performance.

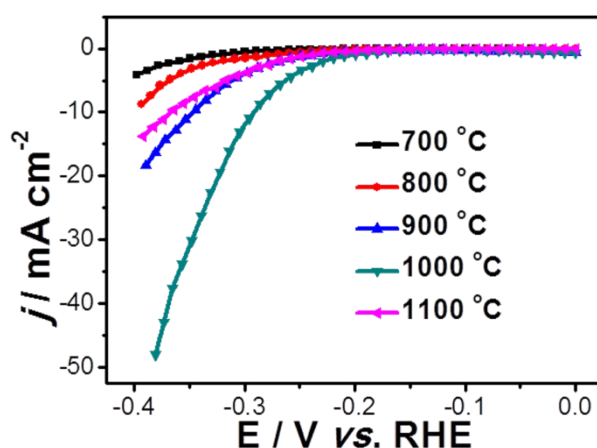


Fig. S9 Steady-state polarization curves of samples activated by KF sintered at different temperatures for HER in 1 M HClO₄ at 25 °C.

Steady-state curves of NFGNS for HER in different *pH* ranges were shown in Fig. S10. NFGNS electrocatalyst exhibits consistent overpotentials (~ 150 mV) for HER at alkaline and acidic medium. NFGNS shows a better catalytic activity for HER in acidic medium with a current densities of (-) 47.8 mA cm⁻², much larger than that in alkaline medium (-23.6 mA cm⁻²). However, NFGNS electrocatalyst almost exhibits

no catalytic activity towards HER in neutral medium.

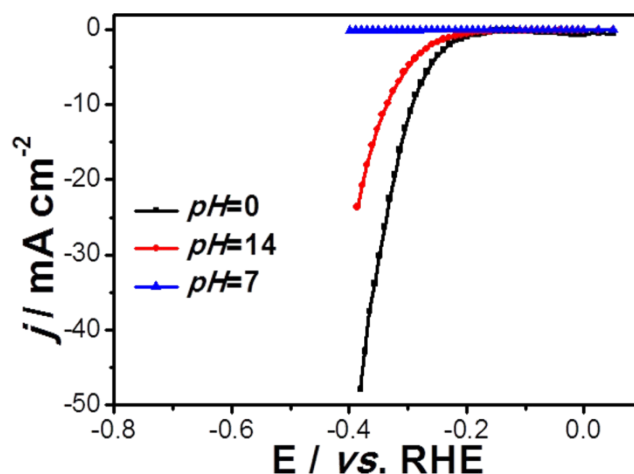


Fig. S10 Steady-state polarization curves of NFPGNS for HER in 1 M HClO₄ ($pH=0$), 1M KOH ($pH=14$) and 1 M phosphate buffered solution (PB) ($pH=7$) at 25 °C.

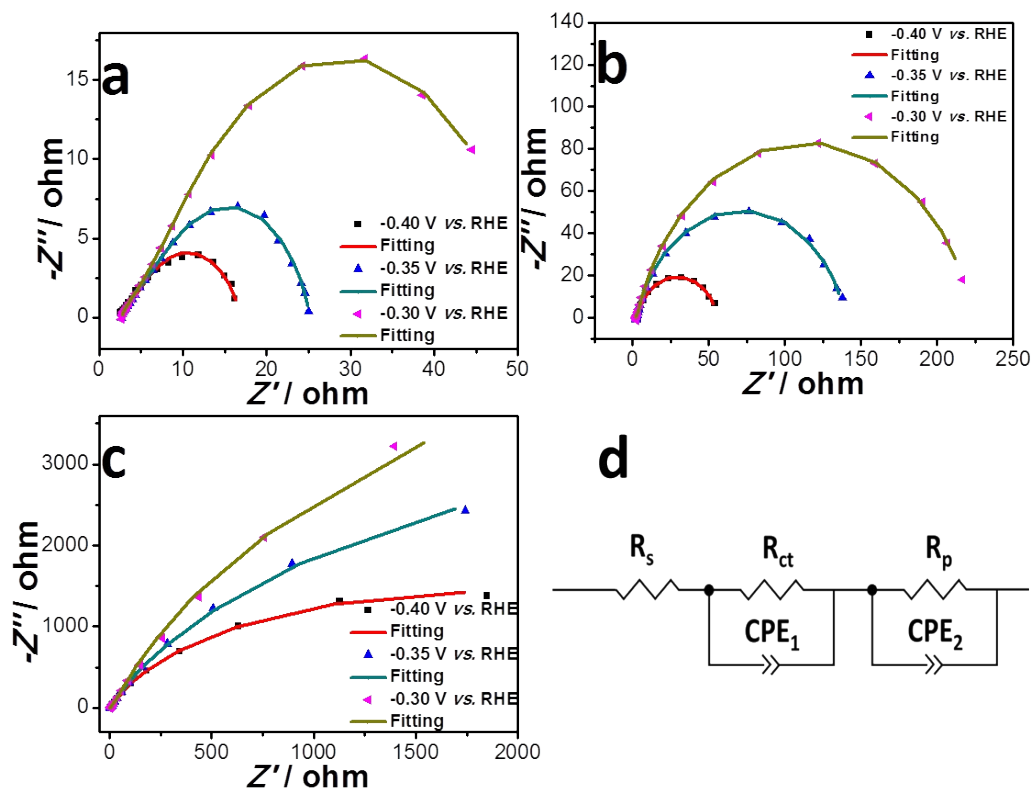


Fig. S11 (a, b and c) Nyquist plots and fittings for impedance response of NG, FC and

CC electrocatalysts toward HER. (d) A two-time constant model for fitting the EIS response of HER on NFPGNS, NG, FC and CC electrocatalysts.

Morphology, composition and structure of NFPGNS after long-term stability test were analysed by SEM, XRD and XPS (Fig. S11-13). SEM images of NFPGNS after long-term stability test exhibit typical sheet-like morphology. The graphite (002) peak was observed on NFPGNS used as catalysts before and after stability test. Meanwhile, there is no other peaks appeared in XRD pattern of sample after stability test. NFPGNS was proved as N and F dual doped structure after stability test according to that XPS peak position was almost identical to the sample used as catalysts before. It means that morphology, structure and composition of NFPGNS are not changed after long-term stability test, indicating superior structural stability.

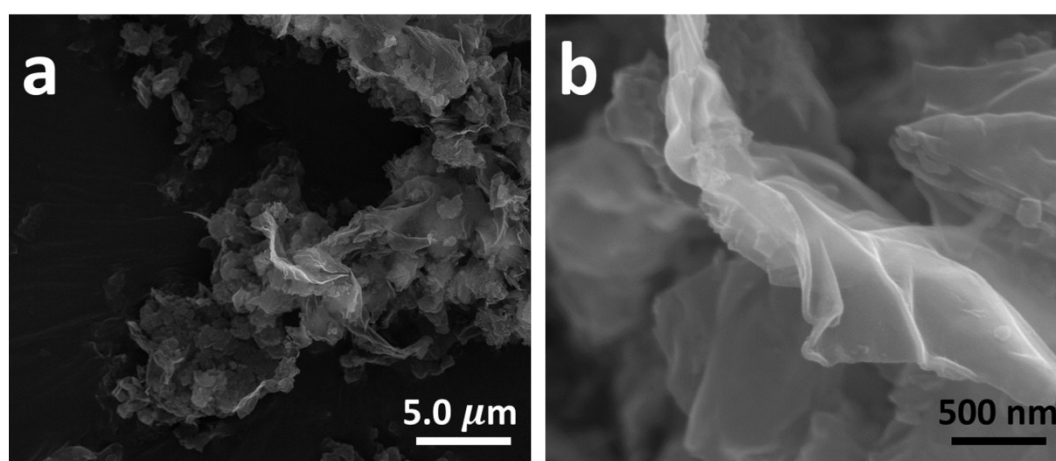


Fig. S12 SEM images of NFPGNS after stability test.

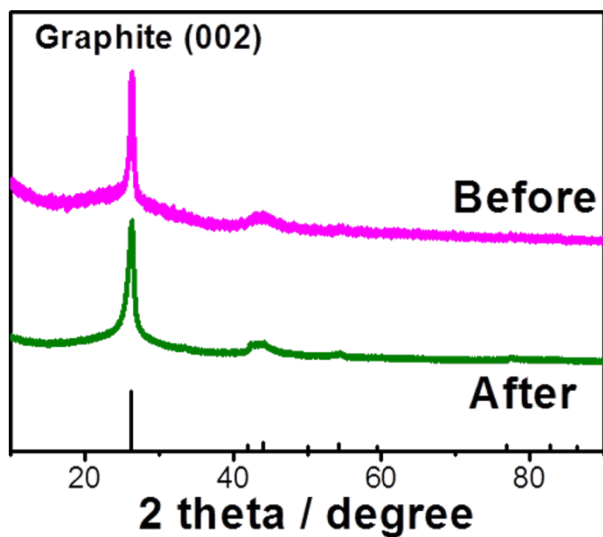


Fig. S13 XRD patterns of NFPNGS used as catalyst before and after long term stability test.

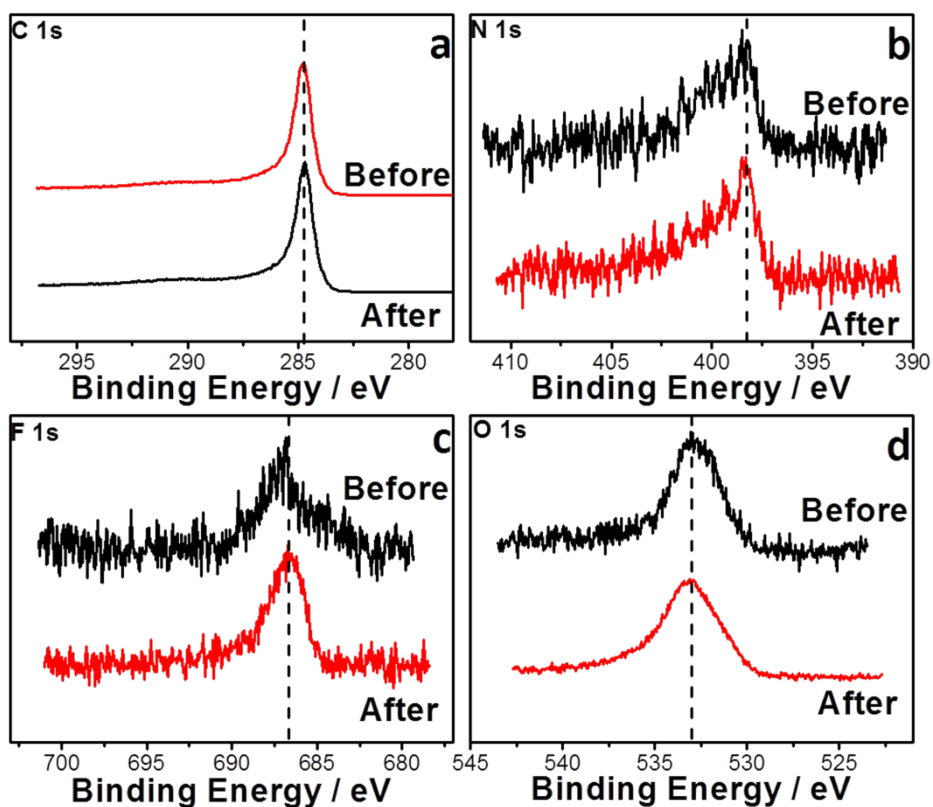


Fig. S14 XPS spectra of NFPNGS used as catalyst before and after long-term stability test.

Mulliken charge distributions of various calculated modes are shown in Fig. S14. In general, Positive charge moved to C sites and negative charge move to N and F sites after N and/or F doped in lattice of graphenebased on higher electronegativities value of N and F than C.

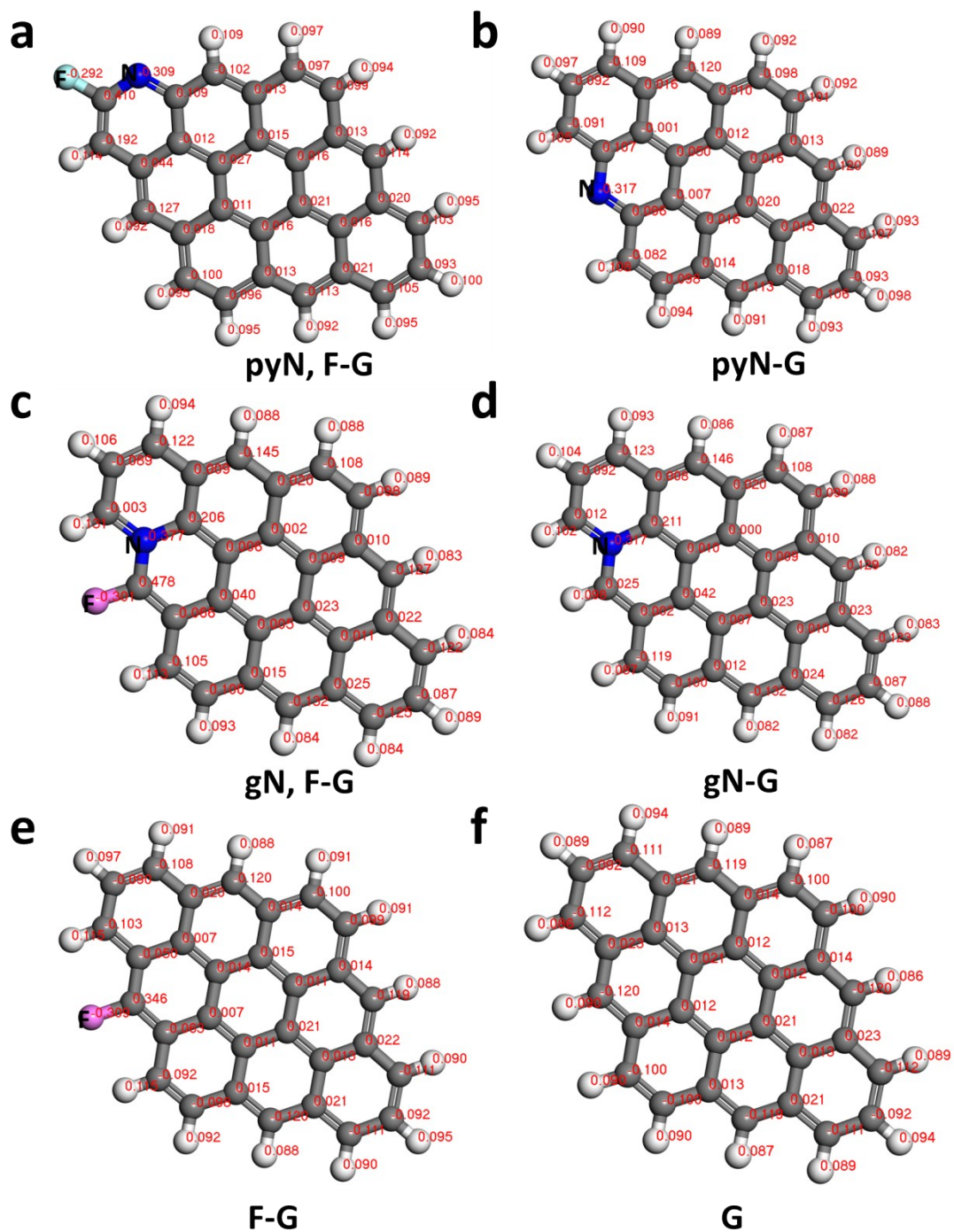


Fig. S15 Atomic structures Mulliken charge distributions of (a) pyN, F-G, (b) pyN-G, (c) gN, F-G, (d) gN-G, (e) F-G and (f) G.

Reference

S1. T. F. Jaramillo, K. P. Jørgensen, J. Bonde, J. H. Nielsen, S. Horch and I.

Chorkendorff, *Science*, 2007, **317**, 100-102.

- S2. J. T. Robinson, J. S. Burgess, C. E. Junkermeier, S. C. Badescu, T. L. Reinecke, F. K. Perkins, M. K. Zalalutdniov, J. W. Baldwin, J. C. Culbertson and P. E. Sheehan, *Nano Lett.*, 2010, **10**, 3001-3005.